ACS OMEGA

http://pubs.acs.org/journal/acsodf

Article

Economical and Easily Obtainable Tools to Manually Develop Lateral Flow Immunoassay Strips

Rowa Y. Alhabbab*

Cite This: *ACS Omega* 2023, 8, 9170−9178

Read Online

ACCESS | Metrics & More | Article Recommendations | Supporting Information

ABSTRACT: The development of inexpensive and highly functional lateral flow devices, which utilize simple and affordable tools, can make them accessible to many populations with insufficient resources. Therefore, this study aims to provide a method to overcome the cost challenges associated with using expensive manufacturing technologies and machinery, particularly during pandemics and upon urgent need. Here, in-house lateral flow strips to detect serum antibodies were developed using low-priced and easily available tools such as adhesive tape and CytoSep layers. The developed lateral flow immunoassay strips presented here produced signals with 93.3 and 96.6% sensitivity for SARS-CoV-2 nucleocapsid protein-specific IgM and IgG antibodies, respectively. The specificity obtained from the developed strips was 96.6% for SARS-CoV-2 nucleocapsid protein-specific IgM and 100% for the IgG antibodies by applying only 5 μL from the serum samples. The proposed design was entirely made manually to ensure a method that would make lateral flow devices available to many populations in need around the globe.

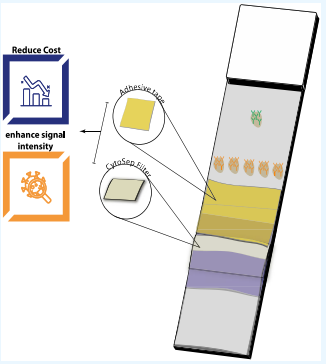

INTRODUCTION

The release of coronavirus (COVID-19)-infected individuals into society based on false-negative results due to insufficient testing greatly influences the spread of COVID-19.[1] Real-time reverse transcriptase polymerase chain reaction (RT-PCR) testing is the standard method to detect COVID-19-infected subjects. Nevertheless, many limitations are associated with RT-PCR testing, including the high testing cost, the necessity of highly trained staff, and expensive testing devices. Enormous efforts have been made to develop point-of-care (POCT) tests to detect coronavirus and help supplement the detection process. The simplicity and low cost associated with POCT, such as lateral flow immunoassay (LFIA) devices, made the assays widely appealing to users and regulatory authorities for their many clinical applications, particularly in the case of the current SARS-CoV-2.[2,3] Although antigen-detecting tests (ATs) like LFIA can produce relatively rapid results without a lab or trained personnel, they are typically less sensitive than the standard molecular and serological methods.[4,5] However, the AT methods used to detect SARS-CoV-2 antigens or antibodies have shown comparable specificity levels to the RT-PCR and enzyme-linked immunosorbent assay (ELISA), respectively.[4,6,7] Several approaches have been applied to enhance the sensitivity and specificity of the available LFIA devices, including signal improvement by utilizing nanoparticles or exterior signal readers.[8,9] Although fluorescent nanoparticles have enhanced the performance and sensitivity of the LFIA testing system,[10−18] these methods require particular readers to interpret the results.

While detecting the SARS-CoV-2 antigens directly by RT-PCR or rapid testing is considered the preferable method, these systems can produce false-negative results for multiple reasons.[19,20] A study by Li et al. found that among every 10 negative RT-PCR subjects, two were proven to be true COVID-19-positive, resulting in a rate of around 20% false-negative RT-PCR results.[20] Factors such as timing and quality of the collected swab samples affect the accuracy of results. Notably, the viral load decreases in the upper respiratory tract over time,[21,22] which frames serological assays' accompaniment with viral detecting tests as essential for result accuracy. Serology can rapidly identify actively infected and immune individuals, helping to minimize the spread of SARS-CoV-2.[23−26] An individual's immunity status to a particular infection can be revealed by detecting the presence of serum-specific IgM and IgG antibodies.[23−26] The standard method to detect humoral responses is ELISA.[27] However, ELISA shares some limitations coupled with RT-PCR testing, including the need for well-trained staff within clinical laboratory settings and a long turnaround time that ranges from 2 to 8 h.[28−30]

Conversely, LFIA assays can be done anywhere without training or needing well-prepared specialized settings. Several well-performing LFIA devices to detect SARS-CoV-2 antigens or humoral responses to COVID-19 have been introduced to the market.[31−33] However, these devices are not always available or affordable in countries with limited resources. Moreover, the manufacturing process involved in producing LFIA requires

Received: October 31, 2022
Accepted: February 20, 2023
Published: March 1, 2023

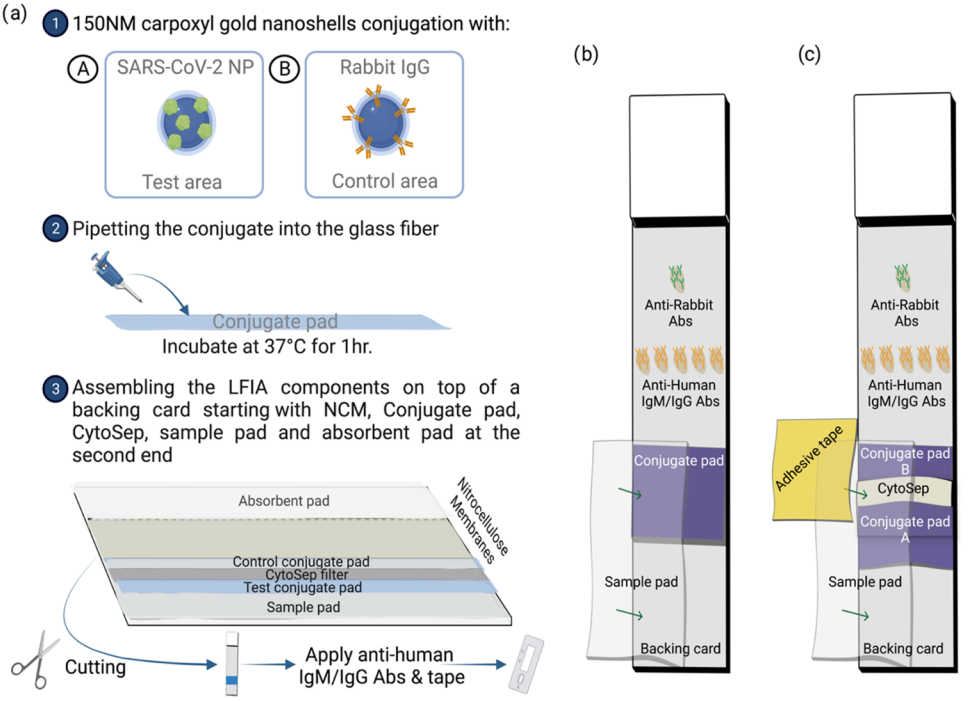

Figure 1. Lateral flow strip preparation. (a) Diagram illustrating the LFIA strip fabrication method, which starts by preparing the conjugate and pipetting the prepared conjugate into the glass fiber. After incubating the conjugate pad at 37 °C for 1 h, the LFIA components are assembled on top of the backing card. Then, the prepared backing card is cut by a pair of scissors, followed by adding the test as well as the control area antibodies by pipette and adhesive tape. Diagram illustrating (b) the components and the design of the standard LFIA strip, while panel (c) illustrates the components and the design of the proposed LFIA strips.

some expensive machinery to print and spray reagents onto different components of the strip. This study describes an equipment-free developing and optimizing method for LFIA strip to manually detect SARS-CoV-2-specific humoral immune responses with low-priced and easily obtainable means using as low as 5 μL from the serum sample. The method presented includes using adhesive tape, CytoSep layers, and commercially available large gold nanoshells——150 nm in size. The developed LFIA strips in this study overcame the need for readers to obtain the results and showed high sensitivity and specificity while maintaining the simplicity of visual coulometric LFIA assays.

RESULTS AND DISCUSSION

LFIA strips were developed successfully to detect SARS-CoV-2-specific IgM and IgG antibodies by assembling all of the essential components required to build up the strip and several additional elements that have been used to develop the proposed strips (Figure 1). Figure 1A illustrates the general steps followed to generate the proposed LFIA strips used in this study. Here, the various components of the strip were fixed on a backing card, which provides the strip with rigidity and makes it easy to handle. The nitrocellulose membrane (NCM) containing the test and the control lines is placed in the middle of the backing card, with the sample pad, conjugate pads, CytoSep layers, and adhesive tape at one end. The second end contains cotton liners to absorb the remaining reagents while clearing up the strip background by maintaining the capillary flow across the membrane (Figure 1B).

Conjugate Pads Preparation and NCM Selection. High-density chopped glass fiber pads were treated with 5% sucrose plus 1% bovine serum albumin (BSA) and 0.5% Tween 20 in Tris buffer (PH 8.5). This treatment ultimately allowed the conjugate pads to fully release the conjugate with high stability, even after one month of storage at 4 °C (Figure S1). After an hour of drying at 37 °C, two sets of conjugate pads were prepared, the test line pads with 150 nm carboxyl gold nanoshells conjugated to SARS-CoV-2-N protein and the control area pads that were saturated with 150 nm carpoxyl gold nanoshells conjugated to normal rabbit control IgG. The pads were then incubated at 37 °C for 2 h and oriented, as illustrated in Figure 1.

Since NCM contains the test and the control lines reagent and delivers the final readout results, the accurate selection of the membrane porosities for LFIA manufacturing is essential. NCM pore size controls the fluid flow of the applied liquid sample throughout the strip and the reaction time. Therefore, three NCMs with different pore sizes (FF80HP, FF120HP, and FF170HP) have been tested.[34] Anti-human IgM or IgG antibodies were pipetted at the test line, while anti-rabbit antibodies were immobilized at the control area. Following the initial optimization steps, all antibodies were immobilized at 0.25 μg/5 mm wide test strip concentrations to detect a clear signal. As shown in Figure 2A, NCM of FF120HP pore size provides significantly higher signal intensities at the test line for the 30 positive serum samples tested with 53.8 and 46.2% increase compared to the FF80HP and the FF170HP membranes, respectively, upon running the same serum samples. In agreement with the literature, the optimal capillary flow time required for the serum sample to incubate with the strip reagents to offer a strong signal is 120 s for every 4 cm moving distance.[35−40] As previously reported, sucrose solution delays the flow rate of the LFIA; thus, the high amount of sucrose used in the in-house running buffer and the slow fluid flow associated with the HH170 membrane upon applying the sample on top of the HH170 membrane present a nonuniform, irregular, and very-slow flow pattern across the membrane.[41]

https://doi.org/10.1021/acsomega.2c07014
ACS Omega 2023, 8, 9170−9178

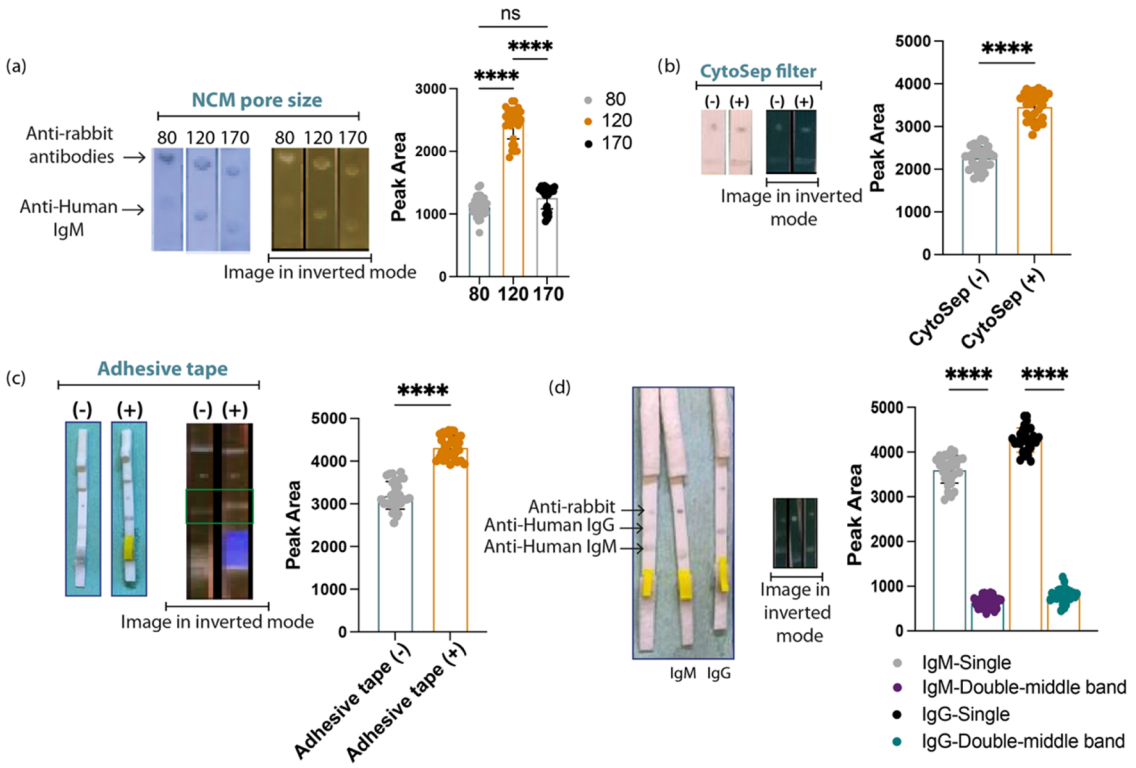

Figure 2. Improving the in-house LFIA test line signals. LFIA strips were developed to include the essential components for a functional test, including a backing card with NCM containing test line (anti-human IgM or IgG antibodies) and control area (anti-rabbit antibodies), two conjugate pads, one with SARS-CoV-2-N protein conjugate and the second with rabbit antibody conjugate, sample pad, and absorbent pad. (a) Photographs (left) of lateral flow strips show the difference in signal intensity at the test line between strips made with NCM of different pore sizes. On the right is a histogram comparing the peak area obtained from the different types of NCM. (b) Photographs (left) of lateral flow strips show the difference in signal intensity at the test line with and without the CytoSep layer and a histogram (right) comparing the peak area obtained from strips with and without the CytoSep layer. (c) Photographs (left) of lateral flow strips show the difference in signal intensity at the test line with or without adhesive tape. On the right is a histogram comparing the peak area obtained from strips with or without adhesive tape. (d) Photographs (left) of lateral flow strips show the difference in signal intensity at the test line upon having two and one test lines. On the right is a histogram comparing the peak area obtained from strips with two and one test lines. Serum samples of known positive ELISA OD readings were dispensed on the manufactured LFIA strips sample loading pad. Statistics were calculated by *t*-test or one-way ANOVA, and * represents significant results. ****$P < 0.0001$ ($n = 30$).

Improving the In-House LFIA Test Line Signals. Having established LFIA strips that can detect SARS-CoV-2 antibodies in patient serum, several components were tested to enhance the test line signals. Various approaches were reported to increase the assay's sensitivity by slowing the flow rate across paper-based POCT membranes. It has been achieved via several methods, including stacking pads,[42] staking flow configurational,[43] and tuneable delay shunts.[44] Here, CytoSep layers purchased from Ahlstrom-Munksjo, which consist of highly pure natural and synthetic fibers, were first examined. The manufacturing company made CytoSep layers to separate and retain blood cells while releasing the plasma components into the LFIA strip sections. Although serum samples were used directly for testing, it was found that adding a CytoSep layer between the test line conjugate pad and control area conjugate pad increases the test line signals significantly (Figure 2B). These results agree with previous reports describing the benefit of adding different stacking pad layers into the test to enhance the performance by decreasing the liquid movement rate.[42,45] Also, it has been reported that thinner stacking pads are better than thicker pads.[42,46] Furthermore, only select materials could be used as a stacking pad since some testing materials retained the flowing components.[42,47] The material used here was as thin as 0.33 mm thick; however, the fiber blend patent belongs to Ahlstrom-Munksjo, and its composition cannot be disclosed. However, it is evident from the results that adding the CytoSep layer has increased the signal intensity by 34.53% compared to the standard LFIA strips. These results indicate that CytoSep is suitable as a stacking pad, can prolong the interaction time, and can release all of the flowing materials successfully. Therefore, CytoSep can be utilized in LFIA strip manufacturing to separate whole blood samples and enhance the test signals upon applying serum samples to the strips.

The observed enhancement in the test line signals upon using CytoSep layers was further improved by slowing the release of the conjugate-serum antibodies into the NCM area. Here, a small piece of waterproof colored adhesive tape was used for this purpose; regardless of the tape provider, the tape adhesive strength was weak upon layering it on the NCM of the LFIA strip. Therefore, the force applied upon adding the sample with the in-house running buffer was sufficient to release the tape end after approximately 3 s, providing a slight delay and more time for the reaction. This slight delay seen upon using this affordable laboratory tape significantly increased the plot area values of the test line for the 30-serum sample mainly by increasing the reaction time and thus enhancing the test signals (Figure 2C).

Furthermore, it was observed that pipetting two test lines on a single NCM considerably decreased the signal intensity of the test line upon testing 30 positive serum samples, particularly for the line placed in the middle between the first test line and the

https://doi.org/10.1021/acsomega.2c07014
ACS Omega 2023, 8, 9170−9178

control area (Figure 2D). One test line to detect anti-human IgM and another to detect anti-human IgG antibodies have been pipetted on the NCM. This weakened signal might be due to the close distance between the test zones that would increase the interference with the identification.[48,49] Although this issue could be resolved by increasing the distance between the test zones, it is more complex upon manually stripping the reagents on top of the NCM with a pipette. Even in the presence of automated manufacturing machinery, many companies chose to construct LFIA devices that detect a single analyte, IgM, or IgG antibodies rather than multiplexing to avoid the risk of interference and to increase the sensitivity of their produced strips.[48] Moreover, adjusting components and conditions of the strips, such as the gold nanoparticles' size, have been reported as essential to increasing the LFIA test sensitivity.[50−52] Here, in consistency with previous reports that have used gold nanoparticles with 35 ± 3 nm rather than using gold nanoparticles of 13 ± 3 nm in diameter to obtain greater signals,[50,53−55] gold nanoshells with a diameter of 150 nm were used to generate test lines with better intensities.

Unlike many introduced methods that require some instruments to prepare the LFIA strip to improve the sensitivity of the LFIA testing, the proposed methods include simple and easily obtainable tools that produce sharp signals in a short amount of time without using any instrumentations to dispense, cut, or illuminate the strips. Therefore, the simple, cost-effective, instrument-free method presented here can help vulnerable populations compensate for some of their demands, mainly since these kits are expensive and always out of stock in many countries.

Testing of the In-House LFIA Strip. LFIA strips were assembled and tested with thirty SARS-CoV-2 negative serum samples or with thirty SARS-CoV-2 positive serum samples collected from COVID-19 RT-PCR-confirmed individuals established of having humoral immune responses upon testing with ELISA. As shown in Figure 3A, the constructed LFIA strip was placed in a commercially made cassette. With the established strong signals obtained with the abovementioned LFIA setup, 5 μL from the SARS-CoV-2 positive serum samples was sufficient to obtain visually clear signals. After 10 to 15 min of applying the serum sample, if only one signal at the control area appears, then the sample is negative, while two signals at the test line and the control area indicate positive results (Figure 3B).

The limits of detection (LODs) were subsequently established for the developed LFIA test. The LODs were obtained using serum specimens with known ELISA OD readings for SARS-CoV-2-N protein IgM and IgG antibodies. Figure S2A shows that the developed strips can detect SARS-CoV-2-N protein-specific IgM and IgG antibodies at OD readings very close to the ELISA cutoff values. The visually seen LOD values for the developed LFIA strips were 0.6 for IgM and 0.45 for IgG. Figure S2B,C shows that the calibration curves generated by plotting the test line peak area versus the ELISA OD readings indicated that the developed LFIA for both IgM and IgG antibodies have a suitable linear dynamic. This data was obtained by plotting the test line peak area versus ELISA OD values from 0.4 to 1 OD. Therefore, the developed LFIA strips can detect COVID-19 antibodies visually and with LODs very similar to the standard assay used to detect antibodies in serum samples.

Prepandemic negative serum samples from 30 healthy individuals and 30 serum samples obtained from RT-PCR

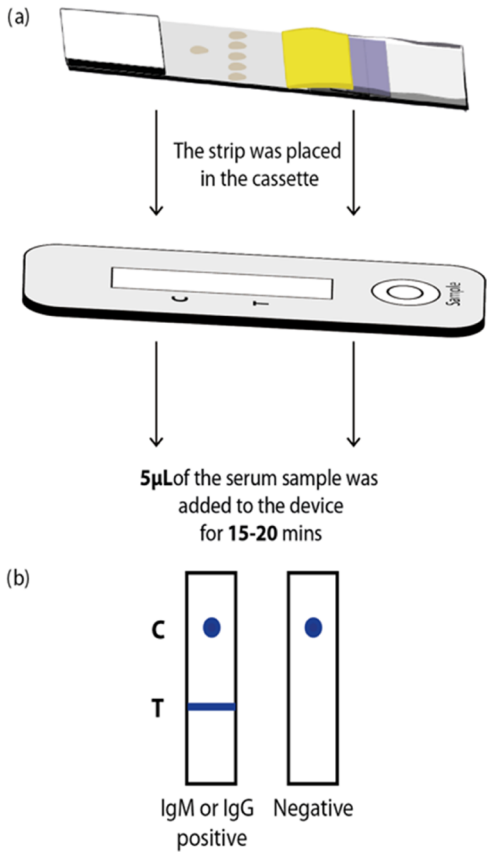

Figure 3. Testing of the in-house LFIA strip. Diagram illustrating the final steps to perform the test, (a) post-preparing the LFIA strips, the strip is placed into the cassette, and then 5 μL of the serum sample is added. After 15 to 20 min, the results can be detected visually. (b) Diagram representing the method of reporting the negative and positive results.

COVID-19 tested individuals with positive humoral immune responses to SARS-CoV-2 upon testing with ELISA (Figure 4A) were used to determine the test sensitivity and specificity. Since LFIA results are qualitative, every IgM or IgG OD reading exceeding the ELISA cutoff value was considered positive. Figure S3 illustrates the IgM and IgG antibody results of the proposed LFIA strips. At the same time, Figure 4B compares the IgM and IgG antibody results obtained by LFIA and ELISA. Although most of the LFIA results were consistent with the ELISA, some false positive and false-negative readouts were detected (Figures 4B and S3). As shown in Figure 4C, the sensitivity of the LFIA test versus ELISA for detecting SARS-CoV-2-N protein-specific IgM antibodies was 93% (95% CI: 79−99%; 28/30) and 97% (95% CI: 83−100%; 29/30) for IgG antibodies. The test specificity was 97% (95% CI: 83−100%; 29/30) for IgM and 100% (95% CI: 87−100%; 0/30) for IgG antibodies (Figure 4D). Moreover, LFIA strips were developed without using the methods presented in this study, and their sensitivity as well as their specificity were tested (Figure S4). Figure S4 shows that the sensitivity of the standard LFIA strips versus ELISA for detecting SARS-CoV-2-N protein-specific IgM antibodies were 80% (95% CI: 62.6−90.5%; 24/30) and 83.3% (95% CI: 66.4−92.6%; 25/30) for IgG antibodies. The test specificity was 86.6% (95% CI: 70−95%; 26/30) for IgM and 90% (95% CI: 74−97%; 0/30) for IgG antibodies (Figure S4). Therefore, these results show that the simple methods proposed here have enhanced the LFIA testing performance. Li and

https://doi.org/10.1021/acsomega.2c07014
ACS Omega 2023, 8, 9170−9178

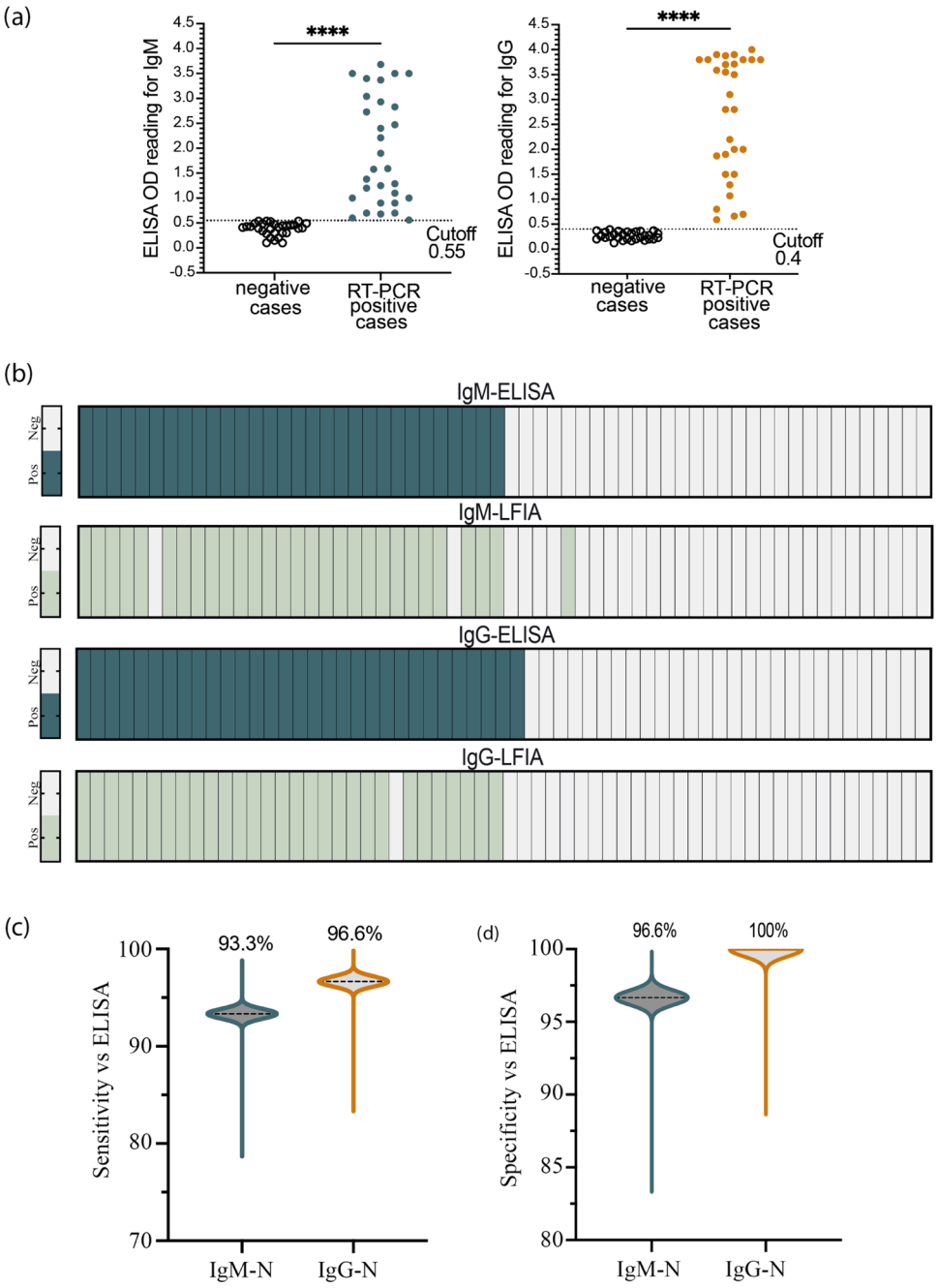

Figure 4. Validation of the in-house LFIA by testing SARS-CoV-2 IgM and IgG-positive and negative samples. Thirty serum specimens obtained from RT-PCR-confirmed SARS-Cov-2 patients and thirty serum samples collected from healthy controls before the pandemic were examined to determine the levels of SARS-CoV-2-N protein IgM and IgG antibodies with ELISA. (a) Plots show ELISA OD reading for SARS-CoV-2 IgM and IgG antibodies. The cutoff threshold for IgM and IgG antibodies was 0.55 and 0.4, respectively. (b) Heat maps showing the results obtained from ELISA and adopted LFIA strips for both SARS-CoV-2-N protein IgM and IgG antibodies. (c, d) Floating plots representing the (c) sensitivity and (d) specificity of the in-house made LFIA strips versus ELISA, the percentages are shown at the top of each plot and the 95% confidence intervals of IgM and IgG antibodies. Statistics were calculated by *t*-test or Wilson/Brown methods, and * represents significant results. ****$P < 0.0001$ ($n = 30$).

colleagues have also shown that LFIA strips, without any improvements, can detect SARS-CoV-2-specific IgM and IgG antibodies with a sensitivity of 88% and specificity of 90.6%.[56] In contrast, Cavalera et al.'s improvement strategy enhanced the coulometric LFIA testing specificity and the sensitivity to reach 100% and 94.6%, respectively. However, their system detected the total SARS-CoV-2-specific antibodies without specifying the class of the antibodies.[57] Applying fluorescent nanoparticles rather than gold nanoparticles has also been used to improve the sensitivity and specificity of the LFIA system. Despite the significant increase in the testing sensitivity and specificity upon using fluorescent nanoparticles, a special reader is required to interpret the results.[10−18] In this study, the LFIA test has been developed with high sensitivity and specificity compared to ELISA, the standard technique for detecting serum antibodies, by applying simple components to the LFIA strips. Thus, these methods provide visual coulometric results with high performance, which could broadly be applied to enhance standard LFIA testing.

https://doi.org/10.1021/acsomega.2c07014
ACS Omega 2023, 8, 9170−9178

CONCLUSIONS

Rapid serological assays to detect antibodies specific for highly infectious agents such as SARS-Cov-2 are essential. Thus, this study showed simple and inexpensive tools to develop LFIA strips that can provide robust and well-defined signals at the test line and require a minimal sample. The abovementioned LFIA test's low cost, minimal development, and performance requirements make it remarkably accessible to many populations, particularly those with insufficient resources. Moreover, using the tools and techniques indicated here in the manufacturing process of the LFIA devices can improve the performance of the available rapid point-of-care serological assays.

EXPERIMENTAL SECTION

Study Design. The LFIA prototype to detect SARS-CoV-2 nucleocapsid (N) protein IgM and IgG antibodies was developed under iterative steps. The capability of the different versions of the strips to detect SARS-CoV-2-N protein IgM- and IgG-specific antibodies was tested using serum samples obtained from SARS-CoV-2 confirmed cases by RT-PCR and tested by ELISA for the presence of SARS-CoV-2-specific IgM and IgG antibodies. All human subjects involved in this study have signed informed consent.

Ethics. The positive and healthy serum samples used in this study were collected based on ethical approval from the Institutional Review Board at the Ministry of Health, Saudi Arabia (IRB Numbers: H-02-J-002). Prepandemic samples were collected 6 months before SARS-CoV-2 from healthy volunteers, and all samples were processed immediately upon arrival to the laboratory, aliquoted, and stored at −80 °C until being used.

Recombinant SARS-CoV-2- N Protein Production. *Escherichia coli* BL21 (DE3) cells were used to express the recombinant SARS-CoV-2-N protein. The protein was then purified using nickel-nitrilotriacetic acid (Ni-NTA) column based on the manufacturer's associated instructions.[58] Subsequently, the positive fractions of N Protein were pooled, and after aliquoting the products, it was stored at −80 °C until being used. The purity of the N protein produced was confirmed using a Western blot with anti-His tag antibodies.

Recombinant SARS-CoV-2-N Protein and Rabbit Antibodies Were Conjugated with 150 nm Carpoxyl Gold Nanoshells. The in-house recombinant SARS-CoV-2-N protein and the normal rabbit control IgG (Sigma-Aldrich, U.K.) were conjugated with the 150 nm carpoxyl gold nanoshells, as illustrated in Figure S5, according to the manufacturer's instructions (nanoComposix, Canada). Here, 8 and 16 μL from ethylcarbodiimide hydrochloride (Sigma-Aldrich) and hydroxysulfosuccinimide (Thermo Fisher) at 10 mg/mL, respectively, were added to 1 mL of 150 nm carpoxyl gold nanoshells and incubated for 30 min at room temperature (RT). After 5 min of centrifugation, 1 mL of reaction buffer (potassium phosphate, pH 7.4) was added, and another spin was performed to wash the particles. Then, 30 μg from the recombinant SARS-CoV-2-N protein or normal rabbit control IgG was added to the reaction and incubated for 1 h at RT. Subsequently, 10 μL of quencher (50% w/v hydroxylamine) was added and incubated for 10 min at RT. After two washes with the reaction buffer, the pellet was resuspended with 1 mL of conjugate buffer (1× Phosphate buffered saline (PBS), 0.5% bovine serum albumin (BSA), 0.5% casein, and 1% Tween 20), and the conjugate was stored at 4 °C.

Lateral Flow Strip Preparation. Each LFIA strip consists of a nitrocellulose membrane (GE Healthcare, Chicago, IL), a sample pad, a test line conjugate pad containing SARS-CoV-2-N protein conjugated to 150 nm carpoxyl gold nanoshells, a control area conjugate pad containing normal rabbit control IgG conjugated to 150 nm carpoxyl gold nanoshells, and an absorbent pad. The nitrocellulose membrane (NCM) contains two manually applied areas using a 0.5−10 μL pipette: a test line area that has goat anti-human IgM or goat anti-human IgG antibodies (Abcam, U.K.) and a control area that contains mouse anti-rabbit antibodies (Abcam, U.K.). After placing the NCM on top of the backing card (DCNovations), all reagents were applied at 0.25 μg/5 mm wide test strip onto the NCM and allowed to dry at RT for 1 h. Then, the conjugate pads, chopped glass with a binder (Ahlstrom-Munksjo), and the CytoSep layer (Ahlstrom-Munksjo) were layered at the NCM first end, as illustrated in Figure 1. The sample pad, chopped glass with a binder (Ahlstrom-Munksjo), was then layered on top of all of the components at this end, and adhesive tape was placed at the joint between the control area conjugate pad and the NCM (Figure 1). The strip also contains the NCM second-end cotton absorbent pad (Ahlstrom-Munksjo).

LFIA Testing Method. Only 5 μL of the serum sample was dispensed on the sample pad, followed by adding 200 μL of running buffer (1× PBS, 1% Tween, 0.05 sodium azide). The samples-conjugate mix then moved via capillary action along the NCM. Antibodies specific for SARS-CoV-2-N protein in the positive pooled serum bind to the conjugate and are captured with the immobilized anti-human IgM or IgG antibodies at the test line. Negative serum migrated via the NCM, and only the normal rabbit control IgG conjugate was captured to the anti-rabbit antibodies in the control area. The remaining reaction mix was streamed to the absorbent pad. In all cases, valid test results required the appearance of a signal at the control area. The presence of two signals, one at the test and a second at the control area, were considered positive results. In contrast, the presence of one signal in the control area was designated as a negative result.

Indirect ELISA Detecting SARS-CoV-2-N Protein IgM and IgG Antibodies. ELISA was performed as previously described by our group.[30] Briefly, recombinant N protein was used at 4 μg mL^{-1} in PBS, and the ELISA plates were coated with the protein at 4 °C overnight. After washing and blocking the plates for 1 h at 37 °C, the plates were washed, and serum samples (1:100) were applied for 1 h at 37 °C. Next, HRP-conjugated anti-human IgM or IgG antibodies were added for 1 h at 37 °C, and the plates were washed. Then, 3,3′,5,5′ tetramethylbenzidine (TMB) substrate was added, and 2 M H_2SO_4 was used to stop the reaction. The absorbance was measured by Synergy 2 multi-detection microplate reader (BioTek, Winooski, VT) at 450 nm.

Statistical Analysis. A smartphone camera photographed the test lines, and the peak values were analyzed by ImageJ software. Notably, the smartphone camera and ImageJ software were used only for experimental validation and were not part of the testing producer. The LOD was obtained from the generated regression analysis and by applying the following equation:

LOD = 3.3 × SD of the y-intercept of the regression line/slop of the regression line. The statistical comparison between two variables was determined using a *t*-test, while more than two variables were compared using one-way ANOVA. Statistical

https://doi.org/10.1021/acsomega.2c07014
ACS Omega 2023, 8, 9170−9178

analysis and graphical presentations were generated using GraphPad Prism version 9.0.2 software (GraphPad Software, Inc., CA).

■ ASSOCIATED CONTENT

Data Availability Statement

The data supporting this study's findings are available upon request from the corresponding author.

Supporting Information

The Supporting Information is available free of charge at https://pubs.acs.org/doi/10.1021/acsomega.2c07014.

Performance of 150 nm carpoxyl gold nanoshells conjugate after one month of storage. The determination of the detection limit of the developed LFIA test. Validation of the in-house LFIA by testing SARS-CoV-2 IgM and IgG-positive and negative samples. Performance of the conventional LFIA strips by testing SARS-CoV-2 IgM and IgG-positive and negative samples. Schematic of the conjugation procedure between the 150 nm carpoxyl gold nanoshells and the targeted proteins (PDF)

■ AUTHOR INFORMATION

Corresponding Author

Rowa Y. Alhabbab − *Vaccines and Immunotherapy Unit, King Fahad Medical Research Center, King Abdulaziz University, Jeddah 21589, Saudi Arabia; Department of Medical Laboratory Sciences, Faculty of Applied Medical Sciences, King Abdulaziz University, Jeddah 21589, Saudi Arabia;* orcid.org/0000-0001-7135-9967; Email: rymalhabbab@kau.edu.sa

Complete contact information is available at: https://pubs.acs.org/10.1021/acsomega.2c07014

Notes

The author declares no competing financial interest.

The data supporting this study's findings are available upon request from the corresponding author.

■ ACKNOWLEDGMENTS

The author would like to thank Community Jameel for supporting this work under Jameel fund for infectious disease research and innovation, grant number (8-4)2120191. The author would also like to thank each and every member working at the Vaccines and Immunotherapy Unit, particularly Professor Anwar Hashem, Professor Adel Abuzenadah and Dr. Sawsan Alamri. The author would also like to thank Yousef Khouqeer for his support in reading this work.

■ REFERENCES

(1) Niu, Y.; Xu, F. Deciphering the power of isolation in controlling COVID-19 outbreaks. *Lancet Global Health* **2020**, *8*, e452−e453.

(2) Nishat, S.; Jafry, A. T.; Martinez, A. W.; Awan, F. R. Paper-based microfluidics: Simplified fabrication and assay methods. *Sens. Actuators, B* **2021**, *336*, No. 129681.

(3) Koczula, K. M.; Gallotta, A. Lateral flow assays. *Essays Biochem.* **2016**, *60*, 111−120.

(4) Gong, F.; Wei, H.-x.; Li, Q.; Liu, L.; Li, B. Evaluation and Comparison of Serological Methods for COVID-19 Diagnosis. *Front. Mol. Biosci.* **2021**, *8*, No. 82405.

(5) Zhang, Y.; Ou, Z.; Yu, Z. Task-Oriented Dialog Systems That Consider Multiple Appropriate Responses under the Same Context. *Proc. AAAI Conf. Artif. Intell.* **2020**, *34*, 9604−9611.

(6) Dinnes, J.; Deeks, J. J.; Berhane, S.; Taylor, M.; Adriano, A.; Davenport, C.; Dittrich, S.; Emperador, D.; Takwoingi, Y.; Cunningham, J.; Beese, S.; Domen, J.; Dretzke, J.; Ferrante di Ruffano, L.; Harris, I. M.; Price, M. J.; Taylor-Phillips, S.; Hooft, L.; Leeflang, M. M. G.; McInnes, M. D. F.; Spijker, R.; Van den Bruel, A. Rapid, point-of-care antigen tests for diagnosis of SARS-CoV-2 infection. *Cochrane Database Syst. Rev.* **2021**, No. CD013705.

(7) Khandker, S. S.; Nik Hashim, N. H. H.; Deris, Z. Z.; Shueb, R. H.; Islam, M. A. Diagnostic Accuracy of Rapid Antigen Test Kits for Detecting SARS-CoV-2: A Systematic Review and Meta-Analysis of 17,171 Suspected COVID-19 Patients. *J. Clin. Med.* **2021**, *10*, No. 3493.

(8) Hsiao, W. W.-W.; Le, T.-N.; Pham, D. M.; Ko, H.-H.; Chang, H.-C.; Lee, C.-C.; Sharma, N.; Lee, C.-K.; Chiang, W.-H. Recent Advances in Novel Lateral Flow Technologies for Detection of COVID-19. *Biosensors* **2021**, *11*, No. 295.

(9) Liu, Y.; Zhan, L.; Qin, Z.; Sackrison, J.; Bischof, J. C. Ultrasensitive and Highly Specific Lateral Flow Assays for Point-of-Care Diagnosis. *ACS Nano* **2021**, *15*, 3593−3611.

(10) Zhou, Y.; Chen, Y.; Liu, W.; Fang, H.; Li, X.; Hou, L.; Liu, Y.; Lai, W.; Huang, X.; Xiong, Y., Development of a rapid and sensitive quantum dot nanobead-based double-antigen sandwich lateral flow immunoassay and its clinical performance for the detection of SARS-CoV-2 total antibodies. *Sens. Actuators, B* **2021**, *343* DOI: 10.1016/j.snb.2021.130139.

(11) Wang, C.; Yang, X.; Gu, B.; Liu, H.; Zhou, Z.; Shi, L.; Cheng, X.; Wang, S. Sensitive and Simultaneous Detection of SARS-CoV-2-Specific IgM/IgG Using Lateral Flow Immunoassay Based on Dual-Mode Quantum Dot Nanobeads. *Anal. Chem.* **2020**, *92*, 15542−15549.

(12) Chen, Z.; Zhang, Z.; Zhai, X.; Li, Y.; Lin, L.; Zhao, H.; Bian, L.; Li, P.; Yu, L.; Wu, Y.; Lin, G. Rapid and Sensitive Detection of anti-SARS-CoV-2 IgG, Using Lanthanide-Doped Nanoparticles-Based Lateral Flow Immunoassay. *Anal. Chem.* **2020**, *92*, 7226−7231.

(13) Shurrab, F. M.; Younes, N.; Al-Sadeq, D. W.; Liu, N.; Qotba, H.; Abu-Raddad, L. J.; Nasrallah, G. K. Performance evaluation of novel fluorescent-based lateral flow immunoassay (LFIA) for rapid detection and quantification of total anti-SARS-CoV-2 S-RBD binding antibodies in infected individuals. *Int. J. Infect. Dis.* **2022**, *118*, 132−137.

(14) Wang, C.; Shi, D.; Wan, N.; Yang, X.; Liu, H.; Gao, H.; Zhang, M.; Bai, Z.; Li, D.; Dai, E.; Rong, Z.; Wang, S. Development of spike protein-based fluorescence lateral flow assay for the simultaneous detection of SARS-CoV-2 specific IgM and IgG. *Analyst* **2021**, *146*, 3908−3917.

(15) Hui, Y. Y.; Chen, O. J.; Lin, H.-H.; Su, Y.-K.; Chen, K. Y.; Wang, C.-Y.; Hsiao, W. W. W.; Chang, H.-C. Magnetically Modulated Fluorescence of Nitrogen-Vacancy Centers in Nanodiamonds for Ultrasensitive Biomedical Analysis. *Anal. Chem.* **2021**, *93*, 7140−7147.

(16) Wang, Z.; Zheng, Z.; Hu, H.; Zhou, Q.; Liu, W.; Li, X.; Liu, Z.; Wang, Y. A point-of-care selenium nanoparticle-based test for the combined detection of anti-SARS-CoV-2 IgM and IgG in human serum and blood. *Lab Chip* **2020**, *20* (22), 4255−4261.

(17) Wang, Z.; Zheng, Z.; Hu, H.; Zhou, Q.; Liu, W.; Li, X.; Liu, Z.; Wang, Y.; Ma, Y. A point-of-care selenium nanoparticle-based test for the combined detection of anti-SARS-CoV-2 IgM and IgG in human serum and blood. *Lab Chip* **2020**, *20*, 4255−4261.

(18) Tjon Kon Fat, E. M.; Abrams, W. R.; Niedbala, R. S.; Corstjens, P. L. A. M.Lateral Flow Sandwich Assay Utilizing Upconverting Phosphor (UCP) Reporters. In *Laboratory Methods in Cell Biology*; Elsevier, 2012; pp 203−234.

(19) Vengesai, A.; Midzi, H.; Kasambala, M.; Mutandadzi, H.; Mduluza-Jokonya, T. L.; Rusakaniko, S.; Mutapi, F.; Naicker, T.; Mduluza, T. A systematic and meta-analysis review on the diagnostic accuracy of antibodies in the serological diagnosis of COVID-19. *Syst. Rev.* **2021**, *10*, No. 155.

(20) Li, D.; Wang, D.; Dong, J.; Wang, N.; Huang, H.; Xu, H.; Xia, C. False-Negative Results of Real-Time Reverse-Transcriptase Polymerase Chain Reaction for Severe Acute Respiratory Syndrome Coronavirus 2: Role of Deep-Learning-Based CT Diagnosis and Insights from Two Cases. *Korean J. Radiol.* **2020**, *21*, 505−508.

(21) Wölfel, R.; Corman, V. M.; Guggemos, W.; Seilmaier, M.; Zange, S.; Muller, M. A.; Niemeyer, D.; Jones, T. C.; Vollmar, P.; Rothe, C.; Hoelscher, M.; Bleicker, T.; Brunink, S.; Schneider, J.; Ehmann, R.; Zwirglmaier, K.; Drosten, C.; Wendtner, C. Virological assessment of hospitalized patients with COVID-2019. *Nature* **2020**, *581*, 465−469.
(22) Jacofsky, D.; Jacofsky, E. M.; Jacofsky, M. Understanding Antibody Testing for COVID-19. *J. Arthroplasty* **2020**, *35*, S74−S81.
(23) Guo, L.; Ren, L.; Yang, S.; Xiao, M.; Chang, D.; Yang, F.; Dela Cruz, C. S.; Wang, Y.; Wu, C.; Xiao, Y.; Zhang, L.; Han, L.; Dang, S.; Xu, Y.; Yang, Q.-W.; Xu, S.-Y.; Zhu, H.-D.; Xu, Y.-C.; Jin, Q.; Sharma, L.; Wang, L.; Wang, J. Profiling Early Humoral Response to Diagnose Novel Coronavirus Disease (COVID-19). *Clin. Infect. Dis.* **2020**, *71*, 778−785.
(24) Zhao, J.; Yuan, Q.; Wang, H.; Liu, W.; Liao, X.; Su, Y.; Wang, X.; Yuan, J.; Li, T.; Li, J.; Qian, S.; Hong, C.; Wang, F.; Liu, Y.; Wang, Z.; He, Q.; Li, Z.; He, B.; Zhang, T.; Fu, Y.; Ge, S.; Liu, L.; Zhang, J.; Xia, N.; Zhang, Z. Antibody Responses to SARS-CoV-2 in Patients With Novel Coronavirus Disease 2019. *Clinical Infectious Diseases* **2020**, *71* (16), 2027−2034.
(25) Stavnezer, J.; Guikema, J. E. J.; Schrader, C. E. Mechanism and Regulation of Class Switch Recombination. *Annu. Rev. Immunol.* **2008**, *26*, 261−292.
(26) Galipeau, Y.; Greig, M.; Liu, G.; Driedger, M.; Langlois, M. A. Humoral Responses and Serological Assays in SARS-CoV-2 Infections. *Front. Immunol.* **2020**, *11*, No. 610688.
(27) Cerda-Kipper, A. S.; Montiel, B. E.; Hosseini, S. Radioimmunoassay and Enzyme-Linked Immunosorbent Assay. In *Reference Module in Chemistry, Molecular Sciences and Chemical Engineering*, Elsevierth ed.; 2018.
(28) Mekonnen, D.; Mengist, H. M.; Derbie, A.; Nibret, E.; Munshea, A.; He, H.; Li, B.; Jin, T. Diagnostic accuracy of serological tests and kinetics of severe acute respiratory syndrome coronavirus 2 antibody: A systematic review and meta-analysis. *Rev. Med. Virol.* **2020**, *31*, No. e2181.
(29) Gong, F.; Wei, H. X.; Li, Q.; Liu, L.; Li, B. Evaluation and Comparison of Serological Methods for COVID-19 Diagnosis. *Front. Mol. Biosci.* **2021**, *8*, No. 682405.
(30) Algaissi, A.; Alfaleh, M. A.; Hala, S.; Abujamel, T. S.; Alamri, S. S.; Almahboub, S. A.; Alluhaybi, K. A.; Hobani, H. I.; Alsulaiman, R. M.; AlHarbi, R. H.; ElAssouli, M. Z.; Alhabbab, R. Y.; AlSaieedi, A. A.; Abdulaal, W. H.; Al-Somali, A. A.; Alofi, F. S.; Khogeer, A. A.; Alkayyal, A. A.; Mahmoud, A. B.; Almontashiri, N. A. M.; Pain, A.; Hashem, A. M. SARS-CoV-2 S1 and N-based serological assays reveal rapid seroconversion and induction of specific antibody response in COVID-19 patients. *Sci. Rep.* **2020**, *10*, No. 16561.
(31) Hashem, A. M.; Alhabbab, R. Y.; Algaissi, A.; Alfaleh, M. A.; Hala, S.; Abujamel, T. S.; ElAssouli, M. Z.; Al-Somali, A. A.; Alofi, F. S.; Khogeer, A. A.; Alkayyal, A. A.; Mahmoud, A. B.; Almontashiri, N. A. M.; Pain, A. Performance of Commercially Available Rapid Serological Assays for the Detection of SARS-CoV-2 Antibodies. *Pathogens* **2020**, *9*, No. 1067.
(32) Rivera-Olivero, I. A.; Henríquez-Trujillo, A. R.; Kyriakidis, N. C.; Ortiz-Prado, E.; Laglaguano, J. C.; Vallejo-Janeta, A. P.; Lozada, T.; Garcia-Bereguiain, M. A. Diagnostic Performance of Seven Commercial COVID-19 Serology Tests Available in South America. *Front. Cell. Infect. Microbiol.* **2022**, *12*, No. 787987.
(33) Dortet, L.; Ronat, J.-B.; Vauloup-Fellous, C.; Langendorf, C.; Mendels, D.-A.; Emeraud, C.; Oueslati, S.; Girlich, D.; Chauvin, A.; Afdjei, A.; Bernabeu, S.; Le Pape, S.; Kallala, R.; Rochard, A.; Verstuyft, C.; Fortineau, N.; Roque-Afonso, A.-M.; Naas, T.; Hanson, K. E. Evaluating 10 Commercially Available SARS-CoV-2 Rapid Serological Tests by Use of the STARD (Standards for Reporting of Diagnostic Accuracy Studies) Method. *J. Clin. Microbiol.* **2021**, *59*, No. e02342-20.
(34) Mahato, K.; Srivastava, A.; Chandra, P. Paper based diagnostics for personalized health care: Emerging technologies and commercial aspects. *Biosens. Bioelectron.* **2017**, *96*, 246−259.
(35) Low, S. C.; Shaimi, R.; Thandaithabany, Y.; Lim, J. K.; Ahmad, A. L.; Ismail, A. Electrophoretic interactions between nitrocellulose membranes and proteins: Biointerface analysis and protein adhesion properties. *Colloids Surf., B* **2013**, *110*, 248−253.
(36) Kaur, M.; Eltzov, E. Optimizing Effective Parameters to Enhance the Sensitivity of Vertical Flow Assay for Detection of *Escherichia coli*. *Biosensors* **2022**, *12*, No. 63.
(37) Borse, V.; Srivastava, R. Process parameter optimization for lateral flow immunosensing. *Mater. Sci. Energy Technol.* **2019**, *2*, 434−441.
(38) Mahato, K.; Srivastava, A.; Chandra, P. Paper based diagnostics for personalized health care: Emerging technologies and commercial aspects. *Biosens. Bioelectron.* **2017**, *96*, 246−259.
(39) Yin, H.-Y.; Fang, T. J.; Li, Y.-T.; Fung, Y.-F.; Tsai, W.-C.; Dai, H.-Y.; Wen, H.-W. Rapidly detecting major peanut allergen-Ara h2 in edible oils using a new immunomagnetic nanoparticle-based lateral flow assay. *Food Chem.* **2019**, *271*, 505−515.
(40) Tang, R.; Alam, N.; Li, M.; Xie, M.; Ni, Y. Dissolvable sugar barriers to enhance the sensitivity of nitrocellulose membrane lateral flow assay for COVID-19 nucleic acid. *Carbohydr. Polym.* **2021**, *268*, No. 118259.
(41) Lutz, B.; Liang, T.; Fu, E.; Ramachandran, S.; Kauffman, P.; Yager, P. Dissolvable fluidic time delays for programming multi-step assays in instrument-free paper diagnostics. *Lab Chip* **2013**, *13*, 2840−2847.
(42) Tsai, T.-T.; Huang, T.-H.; Chen, C.-A.; Ho, N. Y.-J.; Chou, Y.-J.; Chen, C.-F. Development a stacking pad design for enhancing the sensitivity of lateral flow immunoassay. *Sci. Rep.* **2018**, *8*, No. 17319.
(43) Zhang, Y.; Bai, J.; Ying, J. Y. A stacking flow immunoassay for the detection of dengue-specific immunoglobulins in salivary fluid. *Lab Chip* **2015**, *15*, 1465−1471.
(44) Toley, B. J.; McKenzie, B.; Liang, T.; Buser, J. R.; Yager, P.; Fu, E. Tunable-Delay Shunts for Paper Microfluidic Devices. *Anal. Chem.* **2013**, *85*, 11545−11552.
(45) Alam, N.; Tong, L.; He, Z.; Tang, R.; Ahsan, L.; Ni, Y. Improving the sensitivity of cellulose fiber-based lateral flow assay by incorporating a water-dissolvable polyvinyl alcohol dam. *Cellulose* **2021**, *28*, 8641−8651.
(46) Yetisen, A. K.; Akram, M. S.; Lowe, C. R. Paper-based microfluidic point-of-care diagnostic devices. *Lab Chip* **2013**, *13*, 2210−2251.
(47) Atthoff, B.; Hilborn, J. Protein adsorption onto polyester surfaces: Is there a need for surface activation? *J. Biomed. Mater. Res., Part B* **2007**, *80B*, 121−130.
(48) Anfossi, L.; Di Nardo, F.; Cavalera, S.; Giovannoli, C.; Baggiani, C. Multiplex Lateral Flow Immunoassay: An Overview of Strategies towards High-throughput Point-of-Need Testing. *Biosensors* **2019**, *9*, No. 2.
(49) Li, J.; Macdonald, J. Multiplexed lateral flow biosensors: Technological advances for radically improving point-of-care diagnoses. *Biosens. Bioelectron.* **2016**, *83*, 177−92.
(50) Gong, Y.; Hu, J.; Choi, J. R.; You, M.; Zheng, Y.; Xu, B.; Wen, T.; Xu, F. Improved LFIAs for highly sensitive detection of BNP at point-of-care. *Int. J. Nanomed.* **2017**, *12*, 4455−4466.
(51) Posthuma-Trumpie, G. A.; Korf, J.; van Amerongen, A. Lateral flow (immuno)assay: its strengths, weaknesses, opportunities and threats. A literature survey. *Anal. Bioanal. Chem.* **2009**, *393*, 569−582.
(52) Liu, X.; Yang, J.; Li, Q.; Wang, Y.; Wang, Y.; Li, G.; Shi, J.; Ding, P.; Guo, J.; Deng, R.; Zhang, G. A strip test for the optical determination of influenza virus H3 subtype using gold nanoparticle coated polystyrene latex microspheres. *Mikrochim Acta* **2020**, *187*, No. 306.
(53) Aveyard, J.; Mehrabi, M.; Cossins, A.; Braven, H.; Wilson, R. One step visual detection of PCR products with gold nanoparticles and a nucleic acid lateral flow (NALF) device. *Chem. Commun.* **2007**, 4251−4253.
(54) Henderson, K.; Stewart, J. Factors influencing the measurement of oestrone sulphate by dipstick particle capture immunoassay. *J. Immunol. Methods* **2002**, *270*, 77−84.
(55) Laitinen, M. P. A.; Vuento, M. Affinity immunosensor for milk progesterone: identification of critical parameters. *Biosens. Bioelectron.* **1996**, *11*, 1207−1214.

https://doi.org/10.1021/acsomega.2c07014
ACS Omega 2023, 8, 9170−9178

(56) Li, Z.; Yi, Y.; Luo, X.; Xiong, N.; Liu, Y.; Li, S.; Sun, R.; Wang, Y.; Hu, B.; Chen, W.; Zhang, Y.; Wang, J.; Huang, B.; Lin, Y.; Yang, J.; Cai, W.; Wang, X.; Cheng, J.; Chen, Z.; Sun, K.; Pan, W.; Zhan, Z.; Chen, L.; Ye, F. Development and clinical application of a rapid IgM-IgG combined antibody test for SARS-CoV-2 infection diagnosis. *J. Med. Virol.* **2020**, *92*, 1518−1524.
(57) Cavalera, S.; Colitti, B.; Rosati, S.; Ferrara, G.; Bertolotti, L.; Nogarol, C.; Guiotto, C.; Cagnazzo, C.; Denina, M.; Fagioli, F.; Di Nardo, F.; Chiarello, M.; Baggiani, C.; Anfossi, L. A multi-target lateral flow immunoassay enabling the specific and sensitive detection of total antibodies to SARS COV-2. *Talanta* **2021**, *223*, No. 121737.
(58) Hashem, A. M.; Al-Amri, S. S.; Al-Subhi, T. L.; Siddiq, L. A.; Hassan, A. M.; Alawi, M. M.; Alhabbab, R. Y.; Hindawi, S. I.; Mohammed, O. B.; Amor, N. S.; Alagaili, A. N.; Mirza, A. A.; Azhar, E. I. Development and validation of different indirect ELISAs for MERS-CoV serological testing. *J. Immunol. Methods* **2019**, *466*, 41−46.

https://doi.org/10.1021/acsomega.2c07014
ACS Omega 2023, 8, 9170−9178